

## Experimental study of different carbon dust growth mechanisms

C. Arnas<sup>a,\*</sup>, C. Dominique<sup>a</sup>, P. Roubin<sup>a</sup>, C. Martin<sup>a</sup>, C. Laffon<sup>b</sup>,  
P. Parent<sup>b</sup>, C. Brosset<sup>c</sup>, B. Pégourié<sup>c</sup>

<sup>a</sup> Laboratoire PIIM, UMR 6633 CNRS-Universite de Provence, 13397 Marseille, France

<sup>b</sup> LURE, Centre Universitaire Paris-Sud, Bât. 209D, BP 134, F-91898 Orsay cedex, France

<sup>c</sup> Association Euratom-CEA, CEA Cadarache, CEADSM/DRFC, 13108 S<sup>t</sup> Paul Lez Durance, France

### Abstract

Laboratory experiments are proposed to understand the growth mechanisms of spheroid carbon dust grains observed in Tokamaks with inside wall elements in graphite based materials. Different categories of solid grains in the nanometer size range are produced from graphite sputtering in rare gas plasmas. Dense primary particles are observed either individually or in the form of spherical agglomerates. The agglomeration process is likely to be stopped by Coulomb repulsion. Other particulates of higher size and cauliflower texture are formed by atomic-molecule accretion. Examples of these different cases are presented with specific characteristics provided by ex situ diagnostics. A comparison with dust samples collected in Tore Supra or observed in other Tokamaks is proposed.

© 2004 Elsevier B.V. All rights reserved.

PACS: 52.40.HF; 52.25.Vy; 61.46.+w

Keywords: Sputtering; Amorphous carbon; Graphite; Spectroscopy; Tore Supra

### 1. Introduction

Graphite-based walls of fusion devices undergo chemical and physical erosion. The carbon redeposition is not homogeneous and reveals the presence of particulates with a wide range of size and shape [1]. The aim of this work is to get insights on the growth mechanisms of spherical particulates in the nanometer scale range, usually observed in the dust samples. Their spherical shape ensures that they are formed in gas phase [2,3]. Their

precursors likely to be molecules [4] originate from the wall chemical and physical erosion. In the carbon vapor, the atom-molecule condensation gives rise to a large amount of  $C_n^{\pm}$  clusters where  $n$  covers a wide range. For instance, fullerenes with  $n = 60$  or  $70$  have been observed in Tore Supra in its divertor configuration [5]. Multiple cluster collisions can then lead to the formation of spherical particulates which may themselves undergo further collisions and form spherical agglomerates as observed in TEXTOR [6] and in our laboratory experiments. The agglomeration phase stops when the surface effective charge of the new aggregate-particulate specie stabilizes at a negative value [7].

Here, two kind of discharges are proposed in order to form different particulates, in different argon plasmas.

\* Corresponding author. Address: case 321, av. Escadrille Normandie, Niemen, Marseille, France.

E-mail address: [arnas@up.univ-mrs.fr](mailto:arnas@up.univ-mrs.fr) (C. Arnas).

In each case, carbon vapors are produced by sputtering. For low pressure discharges, dense smooth shaped particulates are obtained separately or in the form of spherical agglomerates. We calculate the charge threshold from which the agglomeration phase is stopped by Coulomb repulsion. It is also shown that the aggregate size may still increase by surface atomic-molecular accretion. In particular, when the gas pressure is increased, one obtains particulates with a cauliflower shape likely to be due to a reduced mobility of the surface deposited species. Ex situ diagnostics are used to characterize the sizes, morphologies, chemical composition and structure.

## 2. Experimental arrangements

Two different experimental arrangements are considered. The first one consists in a magnetic multipolar cylinder (40 cm length and 30 cm diameter) used to produce DC argon plasmas at the low pressure of  $P_{Ar} = 2 \times 10^{-3}$  mbar. The ionization is assured by primary electrons emitted by hot tungsten filaments. From Langmuir probe and laser induced fluorescence (LIF) measurements, the discharge electron density is  $n_e \sim 10^{15} \text{ m}^{-3}$ , the electron and ion temperatures are  $T_e \sim 1 \text{ eV}$  and  $T_i \sim 0.04 \text{ eV}$ , respectively (ionized fraction  $\sim 10^{-4}$ ). The Ar–Ar collision mean free path is  $L_{Ar-Ar} \sim 4 \text{ cm}$ . The source of carbon is provided by the ion sputtering of a graphite disc (10 cm) placed at the device center and biased at  $-300 \text{ V}$ . Small conductors are set in the plasma or at the device bottom to collect the particulates formed in the plasma.

In the second study, DC glow discharges are performed between two plane electrodes (10 cm diameter) separated by 5 cm. The graphite cathode is negatively biased at  $-650 \text{ V}$  and the filling gas pressure is  $P_{Ar} = 0.6 \text{ mbar}$ . The plasma parameters are:  $n_e \sim 10^{17} \text{ m}^{-3}$  and  $T_e \sim 1 \text{ eV}$  (ionized fraction  $\sim 10^{-4}$ ) with  $L_{Ar-Ar} \sim 120 \mu\text{m}$ . The carbon source is provided by ions and energetic charge exchange (CX) neutral sputtering since the CX length  $\sim 200 \mu\text{m}$  is smaller than sheath thickness (centimeter range). As controlled by optical spectroscopy of the  $C_2$  Swann band,  $C_2$  molecule being a dust precursor, these discharge parameters are optimized for the dust production. Dusts are collected on the grounded anode surface.

## 3. Carbon particulates produced at low pressure

The scanning electron microscopy (SEM) image of Fig. 1 shows a dust collector surface after an exposition of several hours in a multipolar argon plasma. Two successive depositions are observed: a dense layer of primary particles (PP) of size  $\sim 25 \text{ nm}$  and, superimposed, sepa-

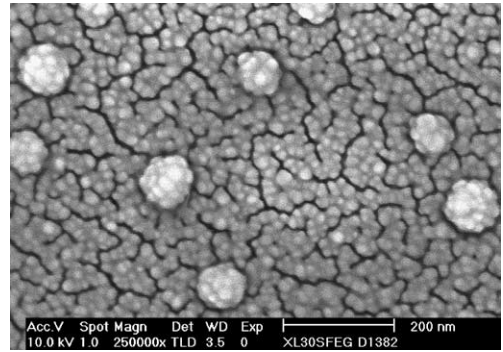


Fig. 1. SEM image of two examples of carbonaceous grains produced in a multipolar argon discharge: a dense layer of primary particles ( $\sim 25 \text{ nm}$ ) and superimposed agglomerates ( $\sim 100 \text{ nm}$ ) of primary particles. The carbon is injected by graphite target sputtering.

rated aggregates of size  $\sim 100 \text{ nm}$  where the PP are still visible. The smooth aspect of the PP surface (at higher magnification) is likely to be explained by the characteristics of the experiment. With an incident ion flux on the graphite target of  $\Gamma_+ = 1.2 \times 10^{19} \text{ m}^{-2} \text{ s}^{-1}$  and an ion energy of  $E_+ = 300 \text{ eV}$  (collisionless sheath), the emitted carbon flux is  $\Gamma_C = 2.4 \times 10^{18} \text{ m}^{-2} \text{ s}^{-1}$  (sputtering yield of  $\sim 0.2$ ) with a typical energy of the emitted carbon atoms of  $E_C \sim 3.5 \text{ eV}$  from Thomson's model [8]. Owing to the density of the argon atoms, our numerical simulations show that the carbon atoms are thermalized at a distance of  $\sim 18 \text{ cm}$  (i.e.  $\sim 2/3$  of the size of the device). One can therefore expect that the PP are formed by the deposition of particles of significant kinetic energy. This favors the formation of dense, uniform surfaces through a high surface mobility of the deposited species.

As long as the size of the PP remains small, their electric charge fluctuates, being alternatively positive and negative. This is why they deposit as a continuous layer on the collector and why they can form larger particulates by agglomeration. With increasing size, the condition of zero net current at their surface applies and their charge stabilizes at a negative value. The particulates are then analogous to small Langmuir probes (of size much smaller than the linearized Debye length) whose equilibrium charge can be calculated by the standard Orbital Motion Limited (OML) model [9,10]. In this calculation, caution must be paid to take into account not only the electron and ion fluxes of the background plasma, but also the flux of primary electrons emitted by the tungsten filaments (for a detailed calculation, see Ref. [7]). One finds then an agglomerate charge of  $Q \sim -2.3 \times 10^{-17} \text{ C}$  ( $145 e^-$ ), high enough to stop the agglomeration phase and to lead to a separated deposition because of mutual Coulomb repulsion.

In these conditions (low filling pressure), the dust production rate is low and does not allow to collect

quantities large enough for a detailed analysis. In particular, it was not possible to make a statistical study of the size evolution in function of the time discharge and (or) the injected power. If one restricts to a morphological characterization, it is interesting to note that similar grains were observed in TEXTOR [6]: spherical agglomerates in the micrometer scale range in which the PP (nanometer size range) are visible.

#### 4. Carbon particulates produced in a glow discharge

Fig. 2 shows another example of dust produced after several successive 10 min glow discharges. Due to the high filling pressure (collisional plasma) and to the cathode sputtering by energetic ions and neutrals, both the incoming flux of carbon and the dust production rate are large. The carbon flux estimated from the total weight of the grain layer on the anode is:  $\Gamma_C \sim 10^{19} \text{ m}^{-2} \text{ s}^{-1}$ . The collected grains exhibit a cauliflower texture and their average size depends on the glow duration: a shorter discharge produces smaller grains. For 10 min duration, the mean size is 300 nm and their cauliflower shape is the signature of a radial columnar growth [11], originating from atomic-molecular accretion (OML charge of  $Q \sim -7.2 \times 10^{-17} \text{ C}$ , i.e.  $450 e^-$ ). This columnar structure could be due to a limitation of the deposited species mobility [12] since our numerical simulations show that the carbon atoms are thermalized at a distance of  $\sim 0.6 \text{ cm}$  from the cathode. Indeed, a weak kinetic energy of the accreting species can lead to the formation of grains less dense than those discussed in Section 3, the cauliflower texture being never observed at low pressure.

At high pressure, the grain production rate is sufficient for a structure analysis to be performed. Therefore, the powder surface (30 Å depth) structure and chemical bonds were characterized by X-ray Absorption Near Edge Spectroscopy (XANES) [13,14]. The experiments

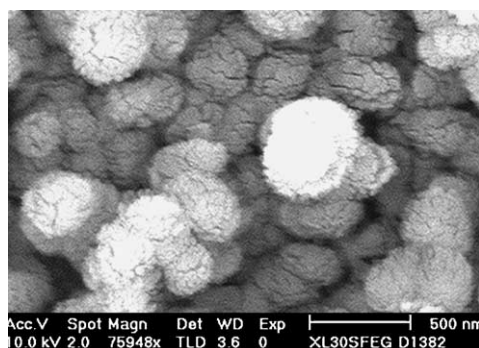


Fig. 2. SEM image of carbonaceous grains ( $\sim 300 \text{ nm}$ ) with a cauliflower texture, produced in a glow discharge. The carbon is injected by graphite cathode sputtering.

were performed in LURE (Super ACO storage ring, Orsay, France) on the SA72 beam line equipped with a high-energy toroidal grating monochromator providing a resolution of  $\sim 300 \text{ meV}$  at the C K edge, in the total electron yield detection mode. The grain surface structure (*Lab sample*) was compared with that of fragments coming from weakly adherent deposits of the upper surface of the Toroidal Pumped Limiteur (TPL) of Tore Supra (TS-TPL-US sample) whose SEM analysis in the range  $0.5\text{--}200 \mu\text{m}$  shows the presence micrometer scale flakes of a porous nature (for more details, see [15]). In both cases, no significant angular signal dependence was observed indicating that the samples are not oriented. A comparison of the two XANES spectra is displayed in Fig. 3(a).

In the case of the TS-TPL-US sample, one observes a peak at 285 eV, signature of the C 1s  $\rightarrow \pi^*$  transition of the  $sp^2$  hybridized carbon in graphite. The continuum structures above 290 eV result from excitonic excitation (291.7 eV) and multiple scattering (MS) resonances within the carbon atoms in the graphite structure [16]. The small peak at 288.5 eV is assigned to C–H bonds, likely

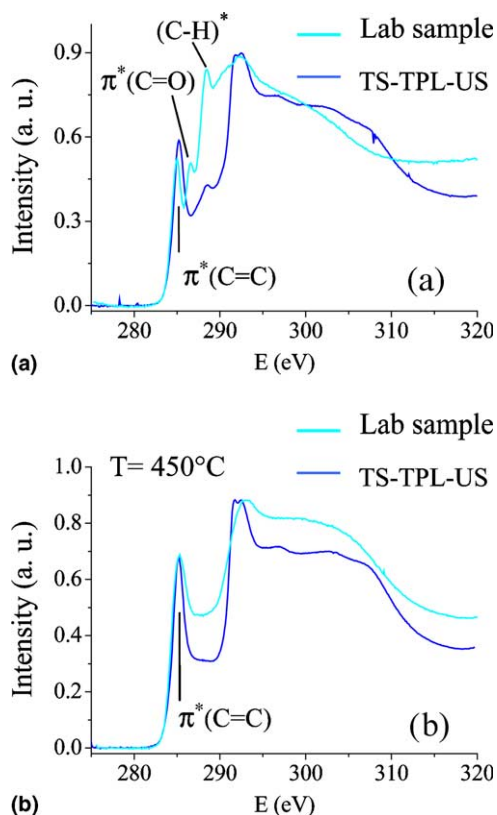


Fig. 3. XANES C K-edge spectra of a dust sample collected in the TPL-US of Tore Supra (December 2002) and grains produced in a glow discharge: (a) without heat, (b) after heating at  $450^\circ \text{C}$ .

due to the cyclohexane solvent used to stick the powder on the sample holder. This spectrum is therefore characteristic of graphite-crystallites at least in the nm range [16].

In the case of the *Lab sample*, the characteristic resonance of unconjugated  $sp^2\pi^*$  (C=C) bond is observed at 284.7 eV [17]. The peaks at 286 eV and 288.5 eV give respectively, the energy position of the  $\pi^*$  (C=O) and  $\sigma^*$  (C–H) transitions. Since optical spectroscopy measurements made during the dust formation never show the presence of oxygen and hydrogen, this could be due to air exposure, indicating a high surface reactivity. The continuum region above 290 eV is made of two broad transitions centered around 292 eV and 300 eV, assigned to the  $\sigma^*$  resonances in  $sp^3$  (C–C) and  $sp^2$  (C=C) hybridization states, respectively. The absence of a MS fine structure in the continuum region as well as the continuum high intensity when compared to that of the  $\pi^*$  (C=C) resonance indicate that the sample is hybridized  $sp^3$  [16]. These characteristics show that the grains produced in glow discharges are essentially made of amorphous tetra-coordinated carbon with some unsaturated C=C groups resulting either from C=C defects in the carbon lattice or from the presence of some dispersed aromatic cycles. The differences observed between the two spectra of Fig. 3(a) can be explained by a difference between the respective sample production mechanisms and by the fact that the TS-TPL-US sample could have undergone heating leading to structural graphitization.

A heating temperature of 450 °C was needed for a total removal of oxygen and hydrogen. As displayed in Fig. 3(b), the  $\sigma^*$  (C–H) signal disappeared in both cases as well as the resonance  $\pi^*$  (C=O) in the *Lab sample* spectrum. In this latter case, the heating also induced a structural change. The shift of the  $\pi^*$  (C=C) from 284.7 to 285 eV clearly shows that graphitization occurred. The intensity of the  $\pi^*$  (C=C) peak also increased when compared to the continuum at higher energies, showing that numerous carbons, initially in a  $sp^3$  configuration, undergone cyclization. The heating also changed the structure of the continuum region which presents now an overall shape close to the TS-TPL-US sample. However, the absence of MS oscillations and of the excitonic structure shows that the dust sample graphitization was limited to a spatial range smaller than several nm [16].

## 5. Conclusion

Laboratory experiments are proposed to understand the growth mechanisms of spherical carbonaceous particulates observed in Tokamak dust samples. Examples can be reproduced when carbon is injected in a plasma discharge by sputtering. The particulates morphology, size, structure, mass density depend on the discharge geome-

try and parameters. At relatively low pressure, nanometer scale primary particles are observed either individually or in the form of spherical agglomerates. The charge threshold from which the agglomeration process is stopped by Coulomb repulsion is established. At higher pressure, the produced grains have a high surface porosity never observed at low pressure, this change being due to a difference in the kinetic energy of the surface deposited species. A comparison was done of the surface structure of laboratory dusts and pieces of carbon deposits from the Toroidal Pumped Limiter of Tore Supra. The observed differences can be explained by different production mechanisms and by the fact that the Tokamak deposits could have undergone heating yielding structural graphitization. Further studies are under way in order to obtain a better understanding of the various particulate morphologies. For instance, we plan to use transmission electron microscopy (TEM) and to complete the XANES structure analysis by Raman spectroscopy. A correlation between the new diagnostics results and the transport of neutral and ion species in our discharges is expected.

## Acknowledgments

This work is supported by the Euratom-CEA Association in the framework of a LRC (Laboratoire de Recherche Conventionné CEA/DSM – Université de Provence PIIM).

## References

- [1] W.J. Carmack, G.R. Smolik, R.A. Ander, R.J. Pawelko, P.B. Hembree, *Fus. Technol.* 34 (1998) 604.
- [2] G.M. Jellum, D.B. Graves, *Appl. Phys. Lett.* 57 (1990) 2077.
- [3] L. Boufendi, A. Plain Blondeau, J.Ph. Blondeau, A. Bouchoule, C. Laure, M. Toogood, *Appl. Phys. Lett.* 60 (1991) 169.
- [4] Ch. Deschenaux, A. Affolter, D. Magni, Ch. Hollenstein, P. Fayet, *J. Phys. D: Appl. Phys.* 32 (1999) 1876.
- [5] Ph. Chappuis, E. Tsitrone, M. Mayne, X. Armand, H. Linke, H. Bolt, D. Petti, J.P. Sharpe, *J. Nucl. Mater.* 290–293 (2001) 245.
- [6] J. Winter, *Plasma Phys. Control. Fus.* 40 (1998) 1201.
- [7] C. Arnas, M. Mikikian, F. Doveil, *Phys. Rev. E* 60 (1999) 7420.
- [8] K. Meyer, I.K. Schuller, C.M. Falco, *J. Appl. Phys.* 52 (1981) 5803.
- [9] M.S. Barnes, J.C. Foster, J.A. O'Neill, O.K. Coultas, *Phys. Rev. Lett.* 68 (1992) 313.
- [10] I.B. Bernstein, I.N. Rabinowitz, *Phys. Fluids* 2 (1959) 112.
- [11] A. Garscadden, B.N. Ganguly, P.D. Haaland, J. Williams, *Plasma Sources Sci. Technol.* 3 (1994) 239.
- [12] J.A. Thornton, *J. Vac. Sci. Technol. A* 4 (1986) 3059.
- [13] Comelli, J. Stohr, J.C. Robinson, W. Jark, *Phys. Rev. B* 38 (1988) 7511.

- [14] C. Martin, C. Brosset, E. Delchambre, C. Laffon, P. Parent, M. Zammouri, P. Roubin, in: 30th EPS Conference on Controlled Fusion and Plasma Physics, ECA Vol. 27A, 2003, PI 158.
- [15] C. Brosset, H. Khodja, in: 16th International Conference on Plasma Surface Interaction in Controlled Fusion Devices, Portland Maine, USA, 2004, P3-8.
- [16] L. Fayette, B. Marcus, M. Mermoux, G. Tourillon, K. Laffon, Ph. Parent, F. Le Normand, *Phys. Rev. B* 57 (1998) 14123.
- [17] J. Stohr, in: R. Gomer (Ed.), *NEXAFS Spectroscopy*, Springer Series in Surface Sciences, Springer-Verlag, Berlin-Heidelberg-New York, Vol. 25, 1996, 107.